

See discussions, stats, and author profiles for this publication at: <https://www.researchgate.net/publication/6389729>

# Theoretical Study on the Second Hyperpolarizabilities of Phenalenyl Radical Systems Involving Acetylene and Vinylene Linkers: Diradical Character and Spin Multiplicity Dependences

ARTICLE in THE JOURNAL OF PHYSICAL CHEMISTRY A · JUNE 2007

Impact Factor: 2.69 · DOI: 10.1021/jp0713662 · Source: PubMed

CITATIONS

61

READS

19

17 AUTHORS, INCLUDING:



Masayoshi Nakano

Osaka University

337 PUBLICATIONS 4,793 CITATIONS

SEE PROFILE



Ryohei Kishi

Osaka University

110 PUBLICATIONS 1,955 CITATIONS

SEE PROFILE



Benoît Champagne

University of Namur

401 PUBLICATIONS 8,753 CITATIONS

SEE PROFILE



Edith Botek

Belgian Institute for Space Aeronomy

104 PUBLICATIONS 2,292 CITATIONS

SEE PROFILE

# Theoretical Study on the Second Hyperpolarizabilities of Phenalenyl Radical Systems Involving Acetylene and Vinylene Linkers: Diradical Character and Spin Multiplicity Dependences

Suguru Ohta,<sup>\*,†</sup> Masayoshi Nakano,<sup>\*,†</sup> Takashi Kubo,<sup>‡</sup> Kenji Kamada,<sup>§</sup> Koji Ohta,<sup>§</sup> Ryohei Kishi,<sup>†</sup> Nozomi Nakagawa,<sup>†</sup> Benoît Champagne,<sup>||</sup> Edith Botek,<sup>||</sup> Akihito Takebe,<sup>†</sup> Shin-ya Umezaki,<sup>†</sup> Masahito Nate,<sup>†</sup> Hideaki Takahashi,<sup>†</sup> Shin-ichi Furukawa,<sup>†</sup> Yasushi Morita,<sup>‡</sup> Kazuhiro Nakasuji,<sup>‡</sup> and Kizashi Yamaguchi<sup>‡</sup>

Department of Materials Engineering Science, Graduate School of Engineering Science, Osaka University, Toyonaka, Osaka 560-8531, Japan, Department of Chemistry, Graduate School of Science, Osaka University, Toyonaka, Osaka 560-0043, Japan, Photonics Research Institute, National Institute of Advanced Industrial Science and Technology (AIST), Ikeda, Osaka 563-8577, Japan, and Laboratoire de Chimie Théorique Appliquée, Facultés Universitaires Notre-Dame de la Paix, rue de Bruxelles, 61, 5000 Namur, Belgium

Received: February 17, 2007; In Final Form: March 8, 2007

We have investigated the static second hyperpolarizabilities ( $\gamma$ ) of the singlet diradical systems with intermediate diradical character involving phenalenyl radicals connected by acetylene and vinylene  $\pi$ -conjugated linkers, **1** and **2**, using the hybrid density functional theory. For comparison, we have also examined the  $\gamma$  values of the closed-shell and pure diradical systems with almost the same molecular size as **1** and **2**. In agreement with our previous prediction of the diradical character dependence of  $\gamma$ , it turns out that the  $\gamma$  values of **1** and **2** are significantly enhanced compared to those of the closed-shell and pure diradical systems. In the present case, distinct differences in  $\gamma$  values are not observed between the two  $\pi$ -conjugated linkers, though the diradical character is found to depend on the kind of linker. Furthermore, we have investigated the spin multiplicity effect on  $\gamma$ . Changing from the singlet to the triplet state, the  $\gamma$  values of the systems with intermediate diradical character in the singlet state are quite reduced, though those of the pure diradical systems are hardly changed. Such spin multiplicity dependence of  $\gamma$  is understood by considering the difference of diradical character between their singlet states together with the Pauli principle. The present results provide a possibility of a novel control scheme of  $\gamma$  for phenalenyl radical systems involving  $\pi$ -conjugated linkers by adjusting the diradical character through the change of the linked position of  $\pi$ -conjugated linkers and the spin multiplicity.

## 1. Introduction

For the past three decades, the research field of nonlinear optics (NLO) has been rapidly developed in pursuit of their potential applications for optoelectronics and photonics.<sup>1–5</sup> Materials with large NLO properties are promising candidates for applications to three-dimensional microfabrication,<sup>6</sup> optical power limiting,<sup>7</sup> optical data processing and storage,<sup>8</sup> photodynamic therapy,<sup>9</sup> and so on. So far, the molecular design of highly active NLO materials has been one of the modern topics from both theoretical and experimental points of view. Indeed, the NLO properties of several materials including inorganic crystals<sup>2,3</sup> and organic molecules<sup>4,10,11</sup> have already been extensively studied. Although inorganic crystals, e.g., LiNbO<sub>3</sub>, KH<sub>2</sub>PO<sub>4</sub>, and BaTiO<sub>3</sub>, are traditional NLO materials, the use has been limited because of the slow NLO responses and the difficulty of dealing with single-crystalline materials. During the past two decades, organic molecular systems with extended

$\pi$ -delocalization have attracted much attention both theoretically and experimentally due to their large susceptibilities, short response time, facility of modification, high laser damage thresholds, and relatively low cost. In particular, structure–property relationships have been deduced for the second hyperpolarizabilities ( $\gamma$ ), which are the microscopic origin of the third-order NLO properties, to realize highly active third-order NLO materials. For example, the extension of  $\pi$ -conjugation length, the introduction of donor/accepter groups<sup>12–14</sup> and the change in charged state<sup>15,16</sup> are primary tuning parameters of  $\gamma$ . Most investigations, however, have focused on the closed-shell systems, though a few pioneering studies on several open-shell systems have been performed from the viewpoint of the hybrid functional materials.<sup>15,17–20</sup>

Recently, we have proposed a novel open-shell molecular-based structure–property relationship for  $\gamma$ : the singlet diradical systems with intermediate diradical characters show a significant enhancement of  $\gamma$  values as compared to the closed-shell and pure diradical systems, and their  $\gamma$  values also change drastically depending on the spin multiplicities.<sup>21</sup> The diradical character ( $y$ ) is an index of the diradical nature of the system and takes a value ranging from 0 to 1, where  $y = 0$  and 1 correspond to the closed-shell and pure diradical systems, respectively. The

\* Authors to whom to correspondence should be addressed. E-mail, mnaka@cheng.es.osaka-u.ac.jp.

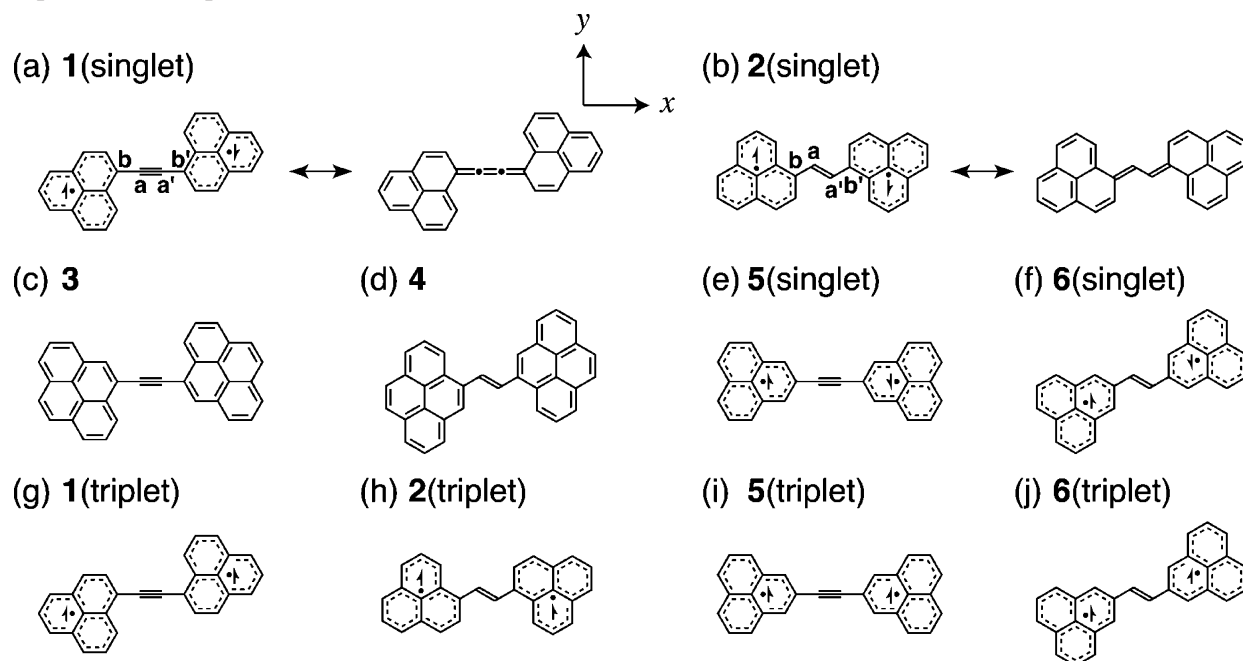
<sup>†</sup> Graduate School of Engineering Science, Osaka University.

<sup>‡</sup> Graduate School of Science, Osaka University.

<sup>§</sup> National Institute of Advanced Industrial Science and Technology (AIST).

<sup>||</sup> Facultés Universitaires Notre-Dame de la Paix.

**CHART 1: Structures of (a) 1,2-Bis(phenalen-1-ylidene)ethene in the Singlet State (1(singlet)), (b) 1,2-Bis(phenalen-1-ylidene)ethane in the Singlet State (2(singlet)), (c) 1,2-Bis(pyren-4-yl)ethyne (3), (d) 1,2-Bis(pyren-4-yl)ethene (4), (e) 1,2-Bis(phenalen-2-yl)ethyne in the Singlet State (5(singlet)), (f) 1,2-Bis(phenalen-2-yl)ethene in the Singlet State (6(singlet)), (g) 1,2-Bis(phenalen-1-ylidene)ethene in the Triplet State (1(triplet)), (h) 1,2-Bis(phenalen-1-ylidene)ethane in the Triplet State (2(triplet)), (i) 1,2-Bis(phenalen-2-yl)ethyne in the Triplet State (5(triplet)), and (j) 1,2-Bis(phenalen-2-yl)ethene in the Triplet State (6(triplet))<sup>a</sup>**



<sup>a</sup> The molecular geometries are optimized at the UB3LYP/6-31G\*\* level of approximation for **1**, **2**, **5**, and **6**, and at the RB3LYP/6-31G\*\* level of approximation for **3** and **4** under the constraint of  $C_{2h}$  symmetry. Main contribution forms and coordinate axis are also shown.

diradical character dependence of  $\gamma$  is explained by using the three-state model for the simplest singlet diradical system, i.e.,  $H_2$  bond dissociation model.<sup>21b,22</sup> For such a model system, a bond dissociation process of the  $H_2$  molecule is classified into three regimes by using the diradical character, i.e., weak-correlation ( $\gamma \sim 0$ ), intermediate-correlation ( $\gamma \sim 0.5$ ), and strong-correlation ( $\gamma \sim 1$ ) regimes, which correspond to the equilibrium-, intermediate-, and long-distance regions, respectively. When the diradical character increases, the transition moment between the first and second excited states increases in contrast to that between the ground and first excited states, which decreases toward a zero value, and also the excitation energies of the first and second excited states decrease and then coincide with each other in the large diradical character region. These features together with the perturbation formula of  $\gamma$  can lead to the diradical character dependence of  $\gamma$ : the  $\gamma$  values attain the maximum in the intermediate diradical character region. In previous studies, we have confirmed the validity of this structure–property relationship using several singlet diradical  $\pi$ -conjugated systems such as *p*-quinodimethane model,<sup>21a</sup> twisted ethylene model<sup>21a</sup> and  $\pi$ -conjugated molecules involving imidazole and triazole rings.<sup>21d</sup>

In addition to these singlet diradical systems, recent development of organic synthesis raises a novel class of thermally stable open-shell systems involving phenalenyl radical rings, which are synthesized by Nakasuji and Kubo.<sup>23</sup> They have proposed a bridging of two phenalenyl radicals by  $\pi$ -conjugated linkers<sup>23a–c</sup> to construct stable phenalenyl-based system. This approach is very fascinating because the variations of the kind and the length of linker molecules are expected to give the variations in diradical character. The phenalenyl radical is also regarded as a building block of various super- and

supramolecules.<sup>24b</sup> Because the  $\gamma$  values of the singlet diradical systems are predicted to show a strong dependence on their diradical characters, phenalenyl-based systems are expected to construct controllable NLO systems. Indeed, we have computationally demonstrated that the  $\pi$ -conjugated hydrocarbons involving diphenalenyl radicals with intermediate diradical characters exhibit a significant enhancement of  $\gamma$  as compared to closed-shell hydrocarbons with similar  $\pi$ -conjugation length.<sup>24</sup>

In this article, we investigate the static longitudinal  $\gamma$  values of linked-type phenalenyl radical compounds, in which two phenalenyl radical rings are connected by acetylene and vinylene linkers, i.e., 1,2-bis(phenalen-1-ylidene)ethene (**1**) and 1,2-bis(phenalen-1-ylidene)ethane (**2**)<sup>23a–c</sup> (Chart 1a,b), by the hybrid density functional theory (DFT) method. To elucidate the diradical character dependences of  $\gamma$ , we also examine the  $\gamma$  values of the systems with small diradical characters, i.e., 1,2-bis(pyren-4-yl)ethyne (**3**) and 1,2-bis(pyren-4-yl)ethene (**4**) (Chart 1c,d), and pure diradical systems, i.e., 1,2-bis(phenalen-2-yl)ethyne (**5**) and 1,2-bis(phenalen-2-yl)ethene (**6**) (Chart 1e,f). Furthermore, the spin multiplicity dependence of  $\gamma$  is investigated by comparing the  $\gamma$  values of **1** (**2**) in the singlet state with those of **1** (**2**) in the triplet state (Chart 1g,h) and the  $\gamma$  values of **5** (**6**) in the singlet state with those of **5** (**6**) in the triplet state (Chart 1i,j). The  $\gamma$  density analysis is performed to elucidate and analyze the spatial contribution of electrons to  $\gamma$ .<sup>15,25</sup> On the basis of these results, we clarify the diradical character and spin multiplicity dependences of  $\gamma$  and discuss a novel control scheme of the third-order NLO properties through the modulation of diradical character by changing the structure, the spin multiplicity and the linked positions of  $\pi$ -conjugated linker in the linked-type diphenalenyl radical systems.

## 2. Theoretical Background and Computational Procedure

### 2.1. Geometrical Structures and Diradical Character.

Chart 1 shows the calculated molecules **1**–**6**, the geometries of which are optimized using the hybrid DFT method, i.e., B3LYP method, with the 6-31G\*\* basis set under the constraint of  $C_{2h}$  symmetry. The B3LYP method is known to reproduce the experimental structures of conjugated diradical systems<sup>26</sup> and our previous study has also shown that the optimized structure for a typical singlet diradical molecule, *p*-quinodimethane, calculated by the B3LYP method is in agreement with that by the quadratic configuration interaction method including all singles and doubles (QCISD),<sup>21a</sup> which significantly improves the description by the Hartree–Fock (HF) method in the weak and intermediate correlation regimes. We therefore employ the spin-unrestricted B3LYP (UB3LYP) method for the open-shell diphenalenyl systems, **1**, **2**, **5**, and **6**, and do the spin-restricted B3LYP (RB3LYP) method for the closed-shell dipyrenyl systems, **3** and **4**, in which the UB3LYP method actually gives the RB3LYP solutions.

So far, numerous efforts have been made to estimate the diradical character of the system<sup>27</sup> and, to this day, the determination of the diradical character attracts the broad interest from the various research field.<sup>28</sup> In this study, we employ the UHF natural orbital (UNO)-based calculation scheme proposed by Yamaguchi et al.<sup>29–31</sup> because this scheme is simple but reproduces well the diradical character calculated by other methods such as the ab initio configuration interaction (CI) method.<sup>26a,30</sup> In this scheme, the diradical character  $y_i$  related to HOMO– $i$  and LUMO+ $i$  is defined by the weight of the doubly excited configuration in the multiconfigurational self-consistent-field (MC–SCF) theory and is formally expressed in the spin-projected UHF (PUHF) as<sup>29–31</sup>

$$y_i = 1 - \frac{2T_i}{1 + T_i^2} \quad (1)$$

where  $T_i$  represents the orbital overlap between the corresponding orbital pairs and is determined by using the occupation numbers ( $n_i$ ) of UNO:

$$T_i = \frac{n_{\text{HOMO}-i} - n_{\text{LUMO}+i}}{2} \quad (2)$$

Because the PUHF diradical characters take values between 0 and 1, which represent the closed-shell and pure diradical states, respectively,  $y_i$  represents the diradical character, i.e., the instability of the chemical bond. The UHF approach is used for the calculation of occupation numbers of NO because the UDFT approach tends to underestimate the diradical character.

**2.2. Second Hyperpolarizability and Hyperpolarizability Density Analysis.** We employ the finite-field (FF) approach<sup>32</sup> to the evaluation of static  $\gamma$ . A power series expansion convention (called B convention<sup>33</sup>) is adopted for the definition of  $\gamma$ . The total energy  $E$  of the system in the presence of static electronic field  $\mathbf{F}$  is expanded as

$$E = E_0 - \sum_i \mu_0^i F^i - \frac{1}{2} \sum_{ij} \alpha_{ij} F^i F^j - \frac{1}{3} \sum_{ijk} \beta_{ijk} F^i F^j F^k - \frac{1}{4} \sum_{ijkl} \gamma_{ijkl} F^i F^j F^k F^l - \dots \quad (3)$$

where  $E_0$  is the total energy of the system in the absence of the applied static electronic field,  $F^i$  indicates the  $i$ th components

( $i = x, y, z$ ) of applied electric field  $\mathbf{F}$  and  $\mu_0^i$ ,  $\alpha_{ij}$ ,  $\beta_{ijk}$ , and  $\gamma_{ijkl}$  represent the permanent dipole moment, polarizability, first hyperpolarizability, and second hyperpolarizability, respectively. From this equation, the static  $\gamma$  can be expressed by

$$\gamma_{ijkl} = -\frac{1}{6} \frac{\partial^4 E}{\partial F^i \partial F^j \partial F^k \partial F^l} \Big|_{\mathbf{F}=0} \quad (4)$$

For all the systems examined in this study, the  $x$ -axis is taken to be the direction of the line joining the middle point between sites **a** and **b** and that between sites **a'** and **b'** (see Chart 1). The origin is chosen to be the molecular center of mass, and the  $x$ – $y$  plane defines the molecular plane. We focus on the longitudinal component of static  $\gamma$  ( $\gamma_{xxxx}$ ) because the longitudinal component is closely related to the  $\pi$ -electron delocalization. The longitudinal components are expected to provide the main contribution of the orientationally averaged second hyperpolarizability ( $\gamma_s$ ) expressed as

$$\gamma_s = (\gamma_{xxxx} + \gamma_{yyyy} + \gamma_{zzzz} + 2\gamma_{xxyy} + 2\gamma_{yyzz} + 2\gamma_{zzxx})/5 \quad (5)$$

We evaluate all components of static  $\gamma$  values contributing to  $\gamma_s$  in eq 5, i.e.,  $\gamma_{iiii}$  and  $\gamma_{iiij}$ , for some systems to investigate the contribution of  $\gamma_{xxxx}$  to  $\gamma_s$ . For the calculation of  $\gamma_{iiii}$  and  $\gamma_{iiij}$ , the fourth-order numerical differentiation formulas are employed:<sup>34</sup>

$$\gamma_{iiii} = -[56E(0) - 39\{E(F^i) + E(-F^i)\} + 12\{E(2F^i) + E(-2F^i)\} - \{E(3F^i) + E(-3F^i)\}]/36(F^i)^4 \quad (6)$$

and

$$\begin{aligned} \gamma_{iiij} = & -[72E(0) - 38\{E(F^i) + E(-F^i) + E(F^j) + E(-F^j)\} + 2\{E(2F^i) + E(-2F^i) + E(2F^j) + E(-2F^j)\} + \\ & 20\{E(F^i, F^j) + E(F^i, -F^j) + E(-F^i, F^j) + E(-F^i, -F^j)\} - \\ & \{E(2F^i, F^j) + E(2F^i, -F^j) + E(-2F^i, F^j) + E(-2F^i, -F^j) + \\ & E(F^i, 2F^j) + E(F^i, -2F^j) + E(-F^i, 2F^j) + E(-F^i, -2F^j)\}]/72(F^i)^2(F^j)^2 \quad (7) \end{aligned}$$

Here,  $E(F^i)$  represents the total energy in the presence of static electric field  $F^i$ , which indicates the  $i$ th components ( $i = x, y, z$ ) of applied electric field  $\mathbf{F}$ , and  $E(F^i, F^j)$  represents that for the applied electric fields  $F^i$  and  $F^j$  with different directions. The values of  $F^i$  giving numerically stable  $\gamma$  values are chosen in the range from 0.0001 to 0.0300 au. The total energy of the system is evaluated within an accuracy of  $10^{-10}$  au, which leads to  $\gamma$  values with sufficient precision for the present study. The  $\gamma$  values are given in atomic units (au): 1.0 au of second hyperpolarizability is equal to  $6.235377 \times 10^{-65} \text{ C}^4 \text{ m}^4 \text{ J}^{-3}$  and  $5.0367 \times 10^{-40} \text{ esu}$ .

The hyperpolarizability density analysis<sup>15,25</sup> is performed to clarify the spatial contribution of electrons to  $\gamma$  value. From the expansions of the charge density function  $\rho(\mathbf{r}, \mathbf{F})$  and of the dipole moment in a power series of applied electronic field  $\mathbf{F}$ ,  $\gamma$  can be expressed by where

$$\gamma_{ijkl} = -\frac{1}{3!} \int r^i \rho_{jkl}^{(3)}(\mathbf{r}) d^3\mathbf{r} \quad (8)$$

$$\rho_{jkl}^{(3)}(\mathbf{r}) = \frac{\partial^3 \rho}{\partial F^j \partial F^k \partial F^l} \Big|_{\mathbf{F}=0} \quad (9)$$



Here,  $r^i$  represents the  $i$ th component of the electron coordinate. This third-order derivative of the electron density with respect to the applied electric fields,  $\rho_{jkl}^{(3)}(\mathbf{r})$ , is referred to as the  $\gamma$  density. The positive and negative values of  $\gamma$  densities multiplied by  $F^3$  correspond to the field-induced increase and decrease in the third-order charge density and induce the third-order dipole moment (third-order polarization) in the direction from positive to negative  $\gamma$  density. The  $\gamma$  density map, therefore, represents the relative phase and magnitude of change in the third-order charge densities between two spatial points with positive and negative  $\gamma$  densities. The relationship between  $\gamma$  and  $\rho_{jkl}^{(3)}(\mathbf{r})$  is explained by considering a simple example: a pair of localized densities with positive and negative values. The sign of the contribution to  $\gamma$  is positive when the direction from positive to negative  $\gamma$  density coincides with the positive direction of the coordinate system. The sign becomes negative in the opposite case. Moreover, the magnitude of the contribution associated with this pair of  $\gamma$  densities is in proportion to the distance between them. The  $\gamma$  densities are calculated for a grid of points using a numerical third-order differentiation formula of the electron densities. The box dimensions ( $-12 \text{ \AA} \leq x \leq 12 \text{ \AA}$ ,  $-10 \text{ \AA} \leq y \leq 10 \text{ \AA}$ ,  $-5 \text{ \AA} \leq z \leq 5 \text{ \AA}$ ) ensure that the  $\gamma$  values obtained by integration are within an accuracy of 2% of the FF results.

We employ the Becke's half and half LYP (BHandHLYP) method<sup>35</sup> using the 6-31G\* basis set for the FF calculation of  $\gamma$ . Our previous study on the *p*-quinodimethane model shows that the spin-unrestricted BHandHLYP (UBHandHLYP) results provide reliable  $\gamma$  values for singlet diradical molecules with intermediate diradical character, whereas the spin-restricted BHandHLYP (RBHandHLYP) results provide reliable  $\gamma$  values for diradical molecules with small diradical character or closed-shell molecules.<sup>21a</sup> Thus, we employ the UBHandHLYP method for the evaluation of  $\gamma$  for **1**, **2**, **5**, and **6**, and the RBHandHLYP method for **3** and **4**.<sup>36</sup> Approximate spin-projection scheme based on the Heisenberg model proposed by Yamaguchi is effective in the calculation of reliable ground-state energies of singlet open-shell systems.<sup>30,37</sup> Indeed, for *p*-quinodimethane model, the  $\gamma$  values obtained by the approximate spin-projection UMP2 (APUMP2) method are improved as compared to those by the UHF and UMP2 methods, which give erroneous results, and are in good agreement with the results obtained at the reliable UCCSD(T) level of theory.<sup>21a</sup> On the other hand, for the H<sub>2</sub> dissociation model, the APUBHandHLYP method is found to provide the maximum  $\gamma$  values at a larger bond distance (corresponding to larger diradical character region) than that at the full-CI (SDCI in this case) level of theory.<sup>22b</sup> This indicates that the spin-projection scheme based on the Heisenberg model tends to cause an overprojection on the  $\gamma$  values at the UBHandHLYP level, which is thus suggested to include some static correlations in spite of the single-reference method. In this study, therefore, we apply the usual UBHandHLYP method (without AP) to the calculation of  $\gamma$  values of the systems with the intermediate and pure diradical characters. Although it is well-known that the use of the extended basis sets such as split-valence plus polarization basis set augmented with a set of *p* and/or *d* diffuse functions on the second-row atoms is necessary for obtaining quantitative  $\gamma$  values for  $\pi$ -conjugated systems,<sup>38</sup> we use the standard 6-31G\* basis set because we focus on the semiquantitative comparison of  $\gamma$  values for the systems with different diradical character. Indeed, our previous study confirms that the  $\gamma$  value of *s*-indaceno[1,2,3-*cd*;5,6,7-*c'd'*]diphenylene (IDPL), which is a singlet polycyclic aromatic diradical system involving two phenalenyl radical rings, using the 6-31G\* basis

**TABLE 1: Diradical Character  $\gamma$  Calculated by the UHF/6-31G\*\* Method and Longitudinal Components of Second Hyperpolarizabilities  $\gamma(\gamma_{xxxx})$  (in the Unit of  $10^3$  a.u.) Calculated by the BHandHLYP/6-31G\* Method<sup>a</sup> for **1**(singlet), **2**(singlet), **3**, **4**, **5**(singlet), **6**(singlet), **1**(triplet), **2**(triplet), **5**(triplet) and **6**(triplet)**

system	$\gamma$	$\gamma [\times 10^3 \text{ au}]$
<b>1</b> (singlet)	0.6525	1568
<b>2</b> (singlet)	0.5184	1889
<b>3</b>	0.1915	360
<b>4</b>	0.2297	324
<b>5</b> (singlet)	0.9993	209
<b>6</b> (singlet)	0.9979	217
<b>1</b> (triplet)		461
<b>2</b> (triplet)		687
<b>5</b> (triplet)		198
<b>6</b> (triplet)		208

<sup>a</sup> The  $\gamma$  values of **1**(singlet), **2**(singlet), **5**(singlet), **6**(singlet), **1**(triplet), **2**(triplet), **5**(triplet), and **6**(triplet) are calculated by the spin-unrestricted BHandHLYP/6-31G\* method, and those of **3** and **4** are done by the spin-restricted BHandHLYP/6-31G\* method.

set is slightly enhanced by 10% compared to that using the 6-31G\*+diffuse *p* ( $\zeta = 0.0523$ ) basis set.<sup>24a</sup> All the calculations in this study are carried out using Gaussian 03.<sup>35</sup>

### 3. Results and Discussion

**3.1. Comparison of  $\gamma$  between Singlet Diphenalenyl Radicals (**1**(singlet) and **2**(singlet)) and Closed-Shell Dipyrrenyl Molecules (**3** and **4**).** Table 1 gives the longitudinal components of static  $\gamma$  ( $\gamma_{xxxx}$ ) values calculated by the FF-UBHandHLYP/6-31G\* method and the diradical characters  $\gamma$  obtained from the UNO/6-31G\*\* for **1**(singlet), **2**(singlet), **3**, and **4**. The  $\gamma$  values of **1**(singlet) and **2**(singlet), which have an intermediate diradical character of  $\gamma = 0.6525$  and  $0.5184$ , amount to  $1568 \times 10^3$  and  $1889 \times 10^3$  au, respectively. Although **3** and **4**, which have  $\pi$ -conjugation lengths similar to those of **1**(singlet) and **2**(singlet), respectively, provide small diradical characters ( $\gamma = 0.1915$  for **3** and  $\gamma = 0.2297$  for **4**), the spin-restricted solutions are found to be stable at the B3LYP and BHandHLYP levels of approximation. This result indicates that **3** and **4** are nearly closed-shell systems or are regarded as closed-shell systems. The  $\gamma$  values of **3** and **4** are  $360 \times 10^3$  and  $324 \times 10^3$  au, respectively, and the ratios of  $\gamma$ , **1**(singlet)/**3** and **2**(singlet)/**4**, are 4.4 and 5.8, respectively. This significant relative increase of  $\gamma$  values for **1**(singlet) and **2**(singlet) is in agreement with our prediction that singlet diradical systems with an intermediate diradical character tend to exhibit larger  $\gamma$  values than the closed-shell systems with a similar  $\pi$ -conjugation length.<sup>21a,21b</sup>

Parts a–d of Figure 1 show the  $\gamma$  density distributions for **1**(singlet), **2**(singlet), **3**, and **4** obtained at the BHandHLYP/6-31G\* level of approximation. In all the systems, i.e., **1**(singlet), **2**(singlet), **3**, and **4**, the main contributions to  $\gamma$  are found to arise from  $\pi$ -electrons, though  $\sigma$ -electrons give small opposite contributions to  $\gamma$ . For **1**(singlet) and **2**(singlet), dominant positive contributions to  $\gamma$  come from the extended positive and negative  $\gamma$  densities well-separately distributed on the left and right phenalenyl radical rings, respectively. Although small opposite (negative) contributions appear in the  $\pi$ -conjugated linker, their contributions are much smaller than those of the both-end phenalenyl ring moieties. The small  $\gamma$  values of **3** and **4** are understood by the significantly reduced  $\gamma$  densities at the both-end pyrenyl ring moieties.

As to the effect of the  $\pi$ -conjugated linkers, i.e., acetylene for **1** and vinylene for **2**, the acetylene linker tends to give larger

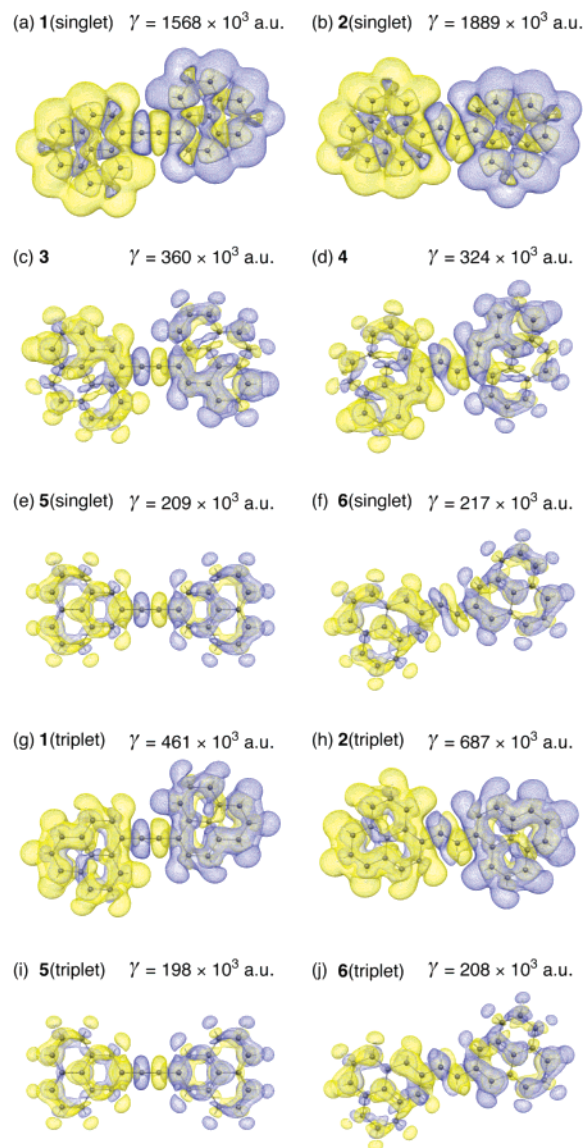


**Figure 1.**  $\gamma$  density distribution calculated at the level of BHandHLYP/6-31G\* approximation and  $\gamma$  values for **1**(singlet), **2**(singlet), **3**, **4**, **5**(singlet), **6**(singlet), **1**(triplet), **2**(triplet), **5**(triplet), and **6**(triplet). The spin-unrestricted method is employed for **1**(singlet), **2**(singlet), **5**(singlet), **6**(singlet), **1**(triplet), **2**(triplet), **5**(triplet), and **6**(triplet), whereas the spin-restricted method is used for **3** and **4**. The yellow and blue meshes represent the positive and negative  $\gamma$  densities with isosurface with  $\pm 100$  au, respectively.

diradical character than the vinylene linker. To clarify the origin of this feature, we compare the frontier orbitals and their energies between **1**(singlet) and **2**(singlet). Parts a and b of Figure 2 show the orbital correlation diagrams for **1**(singlet) and **2**(singlet), respectively, calculated by the RHF/6-31G\* method. The degenerate singly occupied molecular orbitals (SOMOs) of the both-end phenalenyl radical rings are composed of the symmetric and antisymmetric mixings of the SOMOs of isolated phenalenyl radical rings, respectively. The HOMO–LUMO energy gap of **1**(singlet) (4.982 eV) is smaller than that of **2**(singlet) (5.906 eV) because the correlation between the both-end phenalenyl radical rings and  $\pi$ -conjugated linker for **1**(singlet) is slightly smaller than that for **2**(singlet) due to the larger HOMO–LUMO energy gap of acetylene (16.299 eV) than that of vinylene (13.995 eV). In general, the system with a relatively small HOMO–LUMO energy gap tends to give a large diradical character compared to that with a large HOMO–

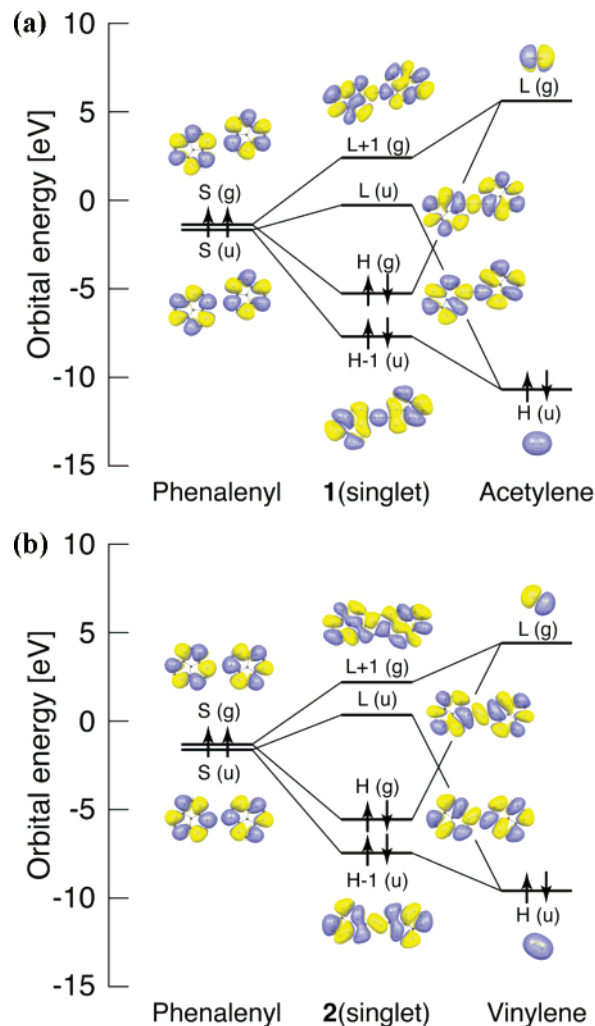


**Figure 2.** Orbital correlation diagrams of (a) **1**(singlet) and (b) **2**(singlet). The frontier orbitals of **1**(singlet) and **2**(singlet) are shown in the center, and those of isolated two phenalenyls and acetylene (vinylene) linker are shown at both ends, respectively. All MOs are calculated by the RHF/6-31G\* method and the yellow and blue surfaces represent the isosurfaces with  $+0.01$  and  $-0.01$  au, respectively. Symbols H, L, and S represent the HOMO, LUMO, and SOMO, respectively, and symbols g and u denote the gerade and ungerade orbitals with respect to the inversion center of the system, respectively.

LUMO energy gap. This is understood as follows. The correct description of the ground state for the system with a small HOMO–LUMO energy gap requires the inclusion of the doubly excited configurations, though the HF ground state configuration is a good approximation to the true ground state in the case of a large HOMO–LUMO energy gap.<sup>21b,39</sup> Such inclusion of the doubly excited configuration in the case of near degenerate HOMO–LUMO energy gap reduces the ionic component overestimated in the HF ground state and thus relatively increases the covalent (diradical) component, leading to the increase of diradical character of the ground state.<sup>21b,39</sup> As a result, we found that the larger HOMO–LUMO energy gap for the acetylene linker than that for the vinylene linker leads to the smaller HOMO–LUMO energy gap of **1**(singlet) and then to a larger diradical character of **1**(singlet) ( $y = 0.6525$ ) as compared to that of **2**(singlet) ( $y = 0.5184$ ). However, we cannot observe a distinct difference in  $\gamma$  values between **1**(singlet) and **2**(singlet) ( $1568 \times 10^3$  au for **1**(singlet) vs  $1889 \times 10^3$  au for **2**(singlet)). This is due to the fact that both the diradical characters of these two molecules lie in the intermediate diradical region.<sup>21a,21b</sup> In the case of longer  $\pi$ -conjugated

**TABLE 2: Components of  $\gamma$ ,  $\gamma_{iii}$ , and  $\gamma_{ijj}$ , and the Orientationally Averaged  $\gamma(\gamma_s)$  ( $10^3$  au) for 1(singlet), 2(singlet), 3, and 4 Calculated by the BHandHLYP/6-31G\* Method<sup>a</sup>**

components [ $\times 10^3$ au]	1(singlet)	2(singlet)	3	4
$\gamma_{xxxx}$	1568	1889	360	324
$\gamma_{yyyy}$	26	5.913	11	2.589
$\gamma_{zzzz}$	0.018	0.018	0.019	0.019
$\gamma_{xxyy}$	140	28	-4.258	41
$\gamma_{yyzz}$	0.068	0.043	0.057	0.071
$\gamma_{zzxx}$	0.354	0.448	0.133	0.099
$\gamma_s$	375	390	73	82

<sup>a</sup> The spin-unrestricted methods are used for 1(singlet) and 2(singlet), and the spin-restricted methods are done for 3 and 4.

linker, more significant difference in  $\gamma$  values is expected between the acetylene and vinylene linker systems because these linkers are predicted to provide a larger difference in HOMO–LUMO energy gap as well as smaller energy gap in the larger chain-length region.

Finally, we investigate the components mainly contributing to the orientationally averaged  $\gamma$  value,  $\gamma_s$ , which is important for the comparison with the experimental values usually measured in solution. The  $\gamma_s$  values and their individual components,  $\gamma_{iii}$  and  $\gamma_{ijj}$ , for 1(singlet), 2(singlet), 3, and 4 calculated by the BHandHLYP/6-31G\* method are listed in Table 2. In all systems, the  $\gamma_{xxxx}$  values are at least 8 times as large as other components, indicating that the  $\gamma_s$  is almost determined by the component of  $\gamma_{xxxx}$ , i.e., the longitudinal component. The present result suggests that our previous prediction<sup>21a,b</sup> is also applicable to the  $\gamma_s$  values, though the amplitudes of off-diagonal components would be somewhat enhanced by the augmentation of the present basis set with diffuse p and/or d functions. In subsequent discussion, we therefore focus on the dominant component of  $\gamma_s$ , i.e., longitudinal component,  $\gamma_{xxxx}$ .

**3.2. Comparison of  $\gamma$  between Singlet Diphenalenyl Radicals (1(singlet) and 2(singlet)) and Pure Diradical Diphenalenyl Molecules (5(singlet) and 6(singlet)).** We examine the  $\gamma$  values and diradical characters of 1(singlet), 2(singlet), 5(singlet), and 6(singlet) to elucidate the difference in  $\gamma$  between the systems with intermediate diradical character and the pure diradical systems. Here, molecules 5(singlet) and 6(singlet) are theoretically designed to be in pure diradical states by linking through  $\pi$ -conjugated linker between the carbon atom sites **a** (with no SOMO distributions) of both-end phenalenyl radical rings (see Figure 3a). This design scheme is verified by examining the highest SOMOs for  $\alpha$  and  $\beta$  spin  $\pi$ -electrons ( $\alpha$ - and  $\beta$ -HSOMOs) of 1(singlet), 2(singlet), 5(singlet), and 6(singlet) calculated by the UBHandHLYP/6-31G\* method (see Figure 3b–e). Apparently, the spatial symmetry of these orbitals is broken. It is found that the  $\alpha$ - and  $\beta$ -HSOMOs of 1(singlet) and 2(singlet) are dominantly distributed on the left- and right-hand side phenalenyl radical rings, respectively, though there is a small distribution of HSOMO in the  $\pi$ -conjugated linker and some invasion to opposite-side phenalenyl ring. This feature exemplifies the intermediate diradical character of 1(singlet) and 2(singlet). In contrast, the  $\alpha$ - and  $\beta$ -HSOMO distributions of 5(singlet) and 6(singlet) are completely separated on the left- and right-hand side phenalenyl radical rings, respectively, which indicates the existence of two radicals localized, respectively, in both-end phenalenyl radical rings, i.e., pure diradical states.

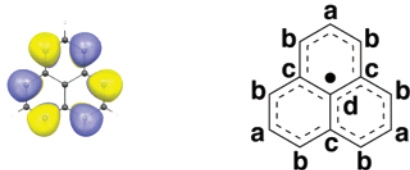
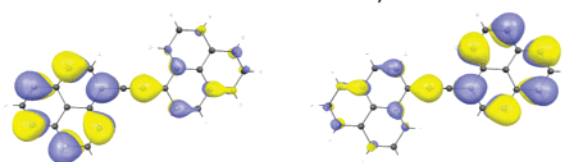
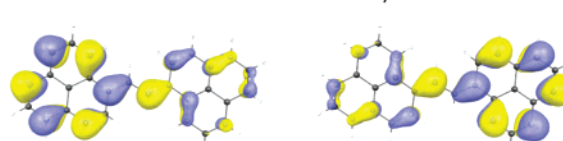
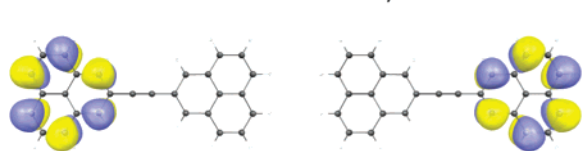
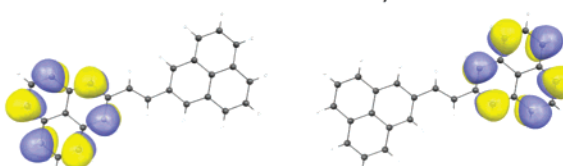
The calculated results of diradical character  $y$  and  $\gamma$  values of 5(singlet) and 6(singlet) are given in Table 1. The pure diradical states of 5(singlet) and 6(singlet) are indicated by the

diradical characters nearly equal to 1:  $y = 0.9993$  for 5(singlet) and 0.9979 for 6(singlet) at the UNO/6-31G\*\* level of approximation. The  $\gamma$  values of 5(singlet) and 6(singlet) calculated by the FF-UBHandHLYP/6-31G\* method are  $209 \times 10^3$  and  $217 \times 10^3$  au, respectively, with the ratios of  $\gamma$ , 1(singlet)/5(singlet) = 7.5 and 2(singlet)/6(singlet) = 8.7. Such significant reduction of  $\gamma$  substantiates our previous prediction<sup>21a,b</sup> that the singlet diradical system with an intermediate diradical character exhibits a larger  $\gamma$  value than the pure diradical system with a similar  $\pi$ -conjugation length. Parts e and f of Figure 1 show the  $\gamma$  density distributions for 5(singlet) and 6(singlet) determined at the UBHandHLYP/6-31G\* level of approximation. The previous features of  $\gamma$  are also well exemplified by the  $\gamma$  density distributions on the both-end phenalenyl rings with dominant contribution: 5(singlet) and 6(singlet) show the significantly reduced densities as compared to those of 1(singlet) and 2(singlet), respectively.

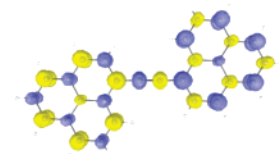
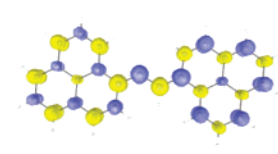
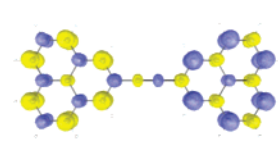
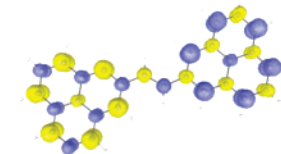
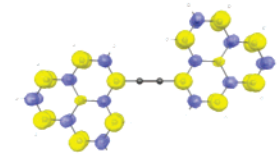
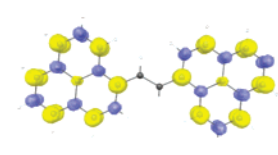
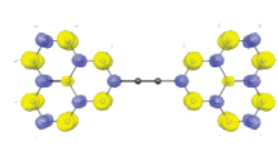
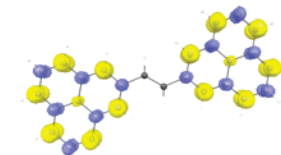
**3.3. Spin Multiplicity Effects on  $\gamma$  for Diphenalenyl Radical Molecules 1, 2, 5, and 6.** The spin multiplicity effect on  $\gamma$  for these diradical systems are investigated using the singlet and triplet states of 1, 2, 5, and 6. It is found from the results by the UBHandHLYP/6-31G\* method with approximately spin-projection scheme<sup>30,37</sup> that the singlet state is slightly more stable than the triplet state for 1 and 2 ( $E_{T-S} (\equiv E_T - E_S) = 2.426$  kcal/mol for 1 and 3.150 kcal/mol for 2), whereas the singlet and triplet states are near-degenerate for 5 and 6 ( $E_{T-S} = 0.8066$  kcal/mol for 5 and 1.190 kcal/mol for 6). This feature is reflected by the intermediate diradical character of singlet 1 and 2 in contrast to the pure diradical character of singlet 5 and 6.<sup>39</sup> The  $\gamma$  values of 1(triplet), 2(triplet), 5(triplet), and 6(triplet) calculated at the UBHandHLYP/6-31G\* level of approximation are listed in Table 1. The  $\gamma$  values of 1(triplet), 2(triplet), 5(triplet), and 6(triplet) are shown to be  $461 \times 10^3$ ,  $687 \times 10^3$ ,  $198 \times 10^3$ , and  $208 \times 10^3$  au, respectively. It turns out that the ratios of  $\gamma$  for the systems with intermediate diradical character, 1(singlet)/1(triplet) and 2(singlet)/2(triplet), are 3.4 and 2.7, respectively, whereas the ratios of  $\gamma$  for the pure diradical system, 5(singlet)/5(triplet) and 6(singlet)/6(triplet), are 1.1 and 1.0, respectively. The significant decrease of  $\gamma$  values in the triplet states compared to those in the singlet states of 1 and 2 are predicted to be caused by the Pauli principle.<sup>21d</sup> In contrast, for pure diradical systems, 5 and 6, such an effect is negligible. This originates in the fact that  $\alpha$ - and  $\beta$ -HSOMOs in the singlet state of pure diradical systems are sufficiently well separated from each other (see Figure 3d,e) in contrast to those of intermediate diradical systems, which have some overlaps between  $\alpha$ - and  $\beta$ -radical orbitals through the  $\pi$ -conjugated linker (see Figure 3b,c). Such well-separated SOMO distributions in the singlet states of 5 and 6 give similar charge density distributions and field-induced polarization to those of the triplet state.

Figure 4 shows the spin density distributions of 1(singlet), 2(singlet), 5(singlet), 6(singlet), 1(triplet), 2(triplet), 5(triplet), and 6(triplet) evaluated at the level of UBHandHLYP/6-31G\* approximation. The spatial distributions concerning  $\alpha$  and  $\beta$  spins in the singlet state are symmetry-broken (spin-polarized) because the spin-unrestricted method is employed. The spin distributions in the singlet state can be interpreted to approximately indicate the feature of spatial correlation between  $\alpha$  and  $\beta$  spins, though such distributions are not observed in the real system. In all the singlet systems, i.e., 1(singlet), 2(singlet), 5(singlet), and 6(singlet), the primary distributions of  $\alpha$  and  $\beta$  spin densities are well separated on the left- and right-hand side phenalenyl rings, respectively, whereas small



(a) Phenalenyl radical  
SOMO(b) **1**(singlet)  $\gamma = 0.6525$   
 $\alpha$ -HSOMO  $\beta$ -HSOMO(c) **2**(singlet)  $\gamma = 0.5184$   
 $\alpha$ -HSOMO  $\beta$ -HSOMO(d) **5**(singlet)  $\gamma = 0.9993$   
 $\alpha$ -HSOMO  $\beta$ -HSOMO(e) **6**(singlet)  $\gamma = 0.9979$   
 $\alpha$ -HSOMO  $\beta$ -HSOMO

**Figure 3.** SOMO of phenalenyl radical (a) and the  $\alpha$ - and  $\beta$ -HSOMO of (b) **1**(singlet), (c) **2**(singlet), (d) **5**(singlet), and (e) **6**(singlet). All MOs are obtained at the UBHandHLYP/6-31G\* level of approximation. The yellow and blue surfaces represent the isosurfaces with +0.025 and -0.025 au, respectively.

(a) **1**(singlet)(b) **2**(singlet)(c) **5**(singlet)(d) **6**(singlet)(e) **1**(triplet)(f) **2**(triplet)(g) **5**(triplet)(h) **6**(triplet)

**Figure 4.** Spin density distributions of (a) **1**(singlet), (b) **2**(singlet), (c) **5**(singlet), (d) **6**(singlet), (e) **1**(triplet), (f) **2**(triplet), (g) **5**(triplet), and (h) **6**(triplet) calculated at the level of UBHandHLYP/6-31G\* approximation. The yellow and blue surfaces represent  $\alpha$  and  $\beta$  spin densities with the isosurfaces with +0.01 and -0.01 au, respectively.

spin densities remain on the  $\pi$ -conjugated linker. Such spin density distributions substantiate that **1**(singlet), **2**(singlet), **5**(singlet), and **6**(singlet) are singlet diradical systems. Moreover, the amplitudes of the spin densities distributed on  $\pi$ -conjugated linker for **5**(singlet) and **6**(singlet) are smaller than those for **1**(singlet) and **2**(singlet), respectively, which supports the fact that **1**(singlet) and **2**(singlet) possess an intermediate diradical character in contrast to **5**(singlet) and **6**(singlet) with pure diradical character. In all the triplet systems, i.e., **1**(triplet), **2**(triplet), **5**(triplet), and **6**(triplet), the spin density distributions are completely separated into the both-end phenalenyl rings and no spin densities are detected on the  $\pi$ -conjugated linker, which originates in the Pauli principle. In contrast to the singlet states, the primary  $\alpha$  spin densities are distributed on the both-end phenalenyl rings of **1**(triplet), **2**(triplet), **5**(triplet), and

**6**(triplet). Spin multiplicity effect on  $\gamma$  mentioned in the previous paragraph is understood by the variation of spin density distributions for the different spin multiplicity. It is found that the separation of the spin densities to the both-end phenalenyl rings of the singlet system with intermediate diradical character, i.e., **1** and **2**, for the change from the singlet to triplet state is more significant than that with pure diradical character, i.e., **5** and **6**. Such significant change in the spin density distributions of **1** and **2**, localization on both phenalenyl rings, for the change from singlet to triplet state provides the significant decrease of field-induced third-order polarization,  $\gamma$ , in the triplet state, whereas the insignificant change of the spin density distributions of **5** and **6** provide the negligible spin multiplicity dependence of  $\gamma$  for pure diradical singlet systems.



The  $\gamma$  density distributions for **1**(triplet), **2**(triplet), **5**(triplet), and **6**(triplet) at the UBHandHLYP/6-31G\* level of approximation are shown in Figure 1g–j. The amplitudes of  $\gamma$  densities on the both-end phenalenyl radical rings for **1**(triplet) and **2**(triplet) are significantly smaller than those for **1**(singlet) and **2**(singlet), whereas the amplitudes of  $\gamma$  densities for **5**(triplet) and **6**(triplet) are almost the same as those for **5**(singlet) and **6**(singlet). These features substantiate the significant spin multiplicity effects on  $\gamma$  values for the intermediate diradical systems, **1** and **2**, and negligible effects on  $\gamma$  for the pure diradical systems, **5** and **6**.

#### 4. Conclusions

We have investigated the second hyperpolarizabilities ( $\gamma$ ) of the singlet diradical systems, **1** and **2**, involving two phenalenyl radical rings connected by two types of  $\pi$ -conjugated linkers, acetylene and vinylene. As references, we examine the closed-shell dipyrrenyl systems, **3** and **4**, and the pure diradical diphenalenyl systems, **5** and **6**, with a different linked position from the case of **1** and **2**. It turns out that the  $\gamma$  values of the singlet diradical systems with intermediate diradical character are significantly enhanced as compared to those with the closed-shell systems and the pure diradical systems. The  $\gamma$  values of the system with intermediate diradical character are 4–6 times enhanced as compared to the corresponding closed-shell systems and 8–9 times compared to the corresponding pure diradical systems. The second hyperpolarizability density analysis clarifies that the enhanced  $\gamma$  values of the systems with intermediate diradical character are dominantly caused by the contributions of both-end phenalenyl radical rings. This suggests the possibility of controlling  $\gamma$  of linked-type diphenalenyl systems by changing the diradical character through adjusting the linked position of  $\pi$ -conjugated linkers. Although the acetylene linker is found to enhance the diradical character compared to the vinylene linker, a distinct difference in  $\gamma$  is not observed for the present systems. The systems with longer  $\pi$ -conjugated linkers are expected to show more significant differences in  $\gamma$  values between the acetylene and vinylene linkers due to enhancing the difference in the degree of  $\pi$ -conjugation between the two linkers as increasing the chain length.

We have also investigated the spin multiplicity effect on  $\gamma$ . On going from the singlet to the triplet state, the  $\gamma$  values of the systems with intermediate diradical character in the singlet state are reduced by a factor of 3, whereas those of the pure diradical systems are hardly changed. This feature arises from the small field-induced polarization of the triplet state originating in the Pauli principle. For pure diradical systems, the well-separated  $\alpha$ - and  $\beta$ -radical orbital distributions in the singlet state, which give similar charge density to that of the triplet state, hardly cause the spin multiplicity effect on  $\gamma$ . These results demonstrate the possibility of spin multiplicity control of the third-order NLO response for the phenalenyl radical systems involving  $\pi$ -conjugated linkers.

At the next stage, we will investigate (i) the dynamic  $\gamma$  of these singlet diradical systems involving the phenalenyl radical rings, (ii) the dependence of  $\gamma$  on the length of  $\pi$ -conjugated linker, and then aim to clarify the third-order NLO properties of the supra- and supermolecules composed of the phenalenyl radical rings and  $\pi$ -conjugated linkers.<sup>24b</sup>

**Acknowledgment.** This work was supported by Grant-in-Aid for Scientific Research (No. 18350007) from Japan Society for the Promotion of Science (JSPS), and Grant-in-Aid for Scientific Research on Priority Areas (No. 18066010) from the

Ministry of Education, Science, Sports and Culture of Japan. B.C. thank the Belgian National Fund for Scientific Research for his Research Director position. E.B. thanks the Interuniversity Attraction Pole on “Supramolecular Chemistry and Supramolecular Catalysis” (IUAP No. P5-03) for her postdoctoral grant. We thank Dr. Takao Tsuneda (The University of Tokyo, Japan) for providing the program code for LC-BLYP. The isosurfaces of spatial distributions of MOs,  $\gamma$  densities and spin densities are plotted using the MACMOLPLT.<sup>40</sup>

**Supporting Information Available:** Diradical characters of dipyrrenyl molecules **3** and **4**, Cartesian coordinates for **1**(singlet), **2**(singlet), **3**, **4**, **5**(singlet), **6**(singlet), **1**(singlet), **2**(singlet), **5**(triplet), and **6**(triplet) optimized at the level of B3LYP/6-31G\*\* approximation and spin expectation values  $\langle S^2 \rangle$  of **1**(singlet), **2**(singlet), **5**(singlet), **6**(singlet), **1**(triplet), **2**(triplet), **5**(triplet), and **6**(triplet) evaluated at the UBHandHLYP/6-31G\* level of approximation. This material is available free of charge via the Internet at <http://pubs.acs.org>.

#### References and Notes

- (1) Boyd, R. W. *Nonlinear Optics*; Academic Press: San Diego, CA, 1992.
- (2) Zyss, J., Ed. *Molecular Nonlinear Optics: Materials, Physics and Devices*; Academic Press: New York, 1994.
- (3) Saleh, B. E. A.; Teich, M. C. *Fundamentals of Photonics*; Wiley: New York, 1991.
- (4) Chemla, D. S.; Zyss, J., Eds. *Nonlinear Optical Properties of Organic Molecules and Crystals*; Academic Press: Orlando, FL, 1987; Vols. 1 and 2.
- (5) Optical Nonlinearities in Chemistry. *Chemical Reviews*; Burland, D. M., Eds.; American Chemical Society: Washington, DC, 1994; Vol. 94.
- (6) (a) Cumpston, B. H.; Ananthavel, S. P.; Barlow, S.; Dyer, D. L.; Ehrlich, J. E.; Erskine, L. L.; Heikal, A. A.; Kuebler, S. M.; Lee, I.-Y. S.; McCord-Maughon, D.; Qin, J.; Röckel, H.; Rumi, M.; Wu, X.-L.; Marder, S. R.; Perry, J. W. *Nature* **1999**, *398*, 51. (b) Kawata, S.; Sun, H.-B.; Tanaka, T.; Takada, T. *Nature* **2001**, *412*, 697. (c) Zhou, W.; Kuebler, S. M.; Braun, K. L.; Yu, T.; Cammack, J. K.; Ober, C. K.; Perry, J. W.; Marder, S. R. *Science* **2002**, *296*, 1106.
- (7) (a) He, G. S.; Bhawalkar, J. D.; Zhao, C. F.; Prasad, P. N. *Appl. Phys. Lett.* **1995**, *67*, 2433. (b) Ehrlich, J. E.; Wu, X. L.; Lee, I.-Y. S.; Hu, Z.-Y.; Röckel, H.; Marder, S. R.; Perry, J. W. *Opt. Lett.* **1997**, *22*, 1843.
- (8) (a) Parthenopoulos, D. A.; Rentzepis, P. M. *Science* **1989**, *245*, 843. (b) Strickler, J. H.; Webb, W. W.; *Opt. Lett.* **1991**, *16*, 1780.
- (9) (a) Bhawalkar, J. D.; Kumar, N. D.; Zhao, C. F.; Prasad, P. N. *J. Clin. Laser Med. Surg.* **1997**, *15*, 201. (b) Frederiksen, P. K.; Jørgensen, M.; Ogilby, P. R. *J. Am. Chem. Soc.* **2001**, *123*, 1215.
- (10) Nalwa, H. S.; Miyata, S., Eds. *Nonlinear Optics of Organic Molecules and Polymers*; CRC Press: Boca Raton, FL, 1997.
- (11) Prasad, P. N.; Williams, D., Eds. *Introduction to Nonlinear Effects in Molecules and Polymers*; J. Wiley: New York, 1991.
- (12) Morley, J. O.; Docherty, V. J.; Pugh, D. J. *Chem. Soc., Perkin Trans. 2* **1987**, 1351.
- (13) Beljonne, D.; Shuai, Z.; Brédas, J. L. *J. Chem. Phys.* **1993**, *98*, 8819.
- (14) Toto, J. L.; Toto, T. T.; de Melo, C. P.; Kirtman, B.; Robins, K. J. *Chem. Phys.* **1996**, *104*, 8586.
- (15) Nakano, M.; Shigemoto, I.; Yamada, S.; Yamaguchi, K. *J. Chem. Phys.* **1995**, *103*, 4175.
- (16) Champagne, B.; Spassova, M.; Jadin, J.-B.; Kirtman, B. *J. Chem. Phys.* **2002**, *116*, 3935.
- (17) Nakano, M.; Yamaguchi, K. *Chem. Phys. Lett.* **1993**, *206*, 285.
- (18) Nakano, M.; Kiribayashi, S.; Yamada, S.; Shigemoto, I.; Yamaguchi, K. *Chem. Phys. Lett.* **1996**, *262*, 66.
- (19) (a) Kamada, K.; Ohta, K.; Nakamura, J.; Yamada, S.; Nakano, M.; Yamaguchi, K. *Mol. Cryst. Liq. Cryst.* **1998**, *315*, 117. (b) Ratera, I.; Marcen, S.; Montant, S.; Ruiz-Molina, D.; Rovira, C.; Veciana, J.; Létard, J.-F.; Freysz, E. *Chem. Phys. Lett.* **2002**, *363*, 245.
- (20) (a) de Melo, C. P.; Fonseca, T. L. *Chem. Phys. Lett.* **1996**, *261*, 28. (b) Nakano, M.; Yamada, S.; Yamaguchi, K. *Bull. Chem. Soc. Jpn.* **1998**, *71*, 845.
- (21) (a) Nakano, M.; Kishi, R.; Nitta, T.; Kubo, T.; Nakasuji, K.; Kamada, K.; Ohta, K.; Champagne, B.; Botek, E.; Yamaguchi, K. *J. Phys. Chem. A* **2005**, *109*, 885. (b) Nakano, M.; Kishi, R.; Ohta, S.; Takebe, A.; Takahashi, H.; Furukawa, S.; Kubo, T.; Morita, Y.; Nakasuji, K.; Yamaguchi, K.; Kamada, K.; Ohta, K.; Champagne, B.; Botek, E. *J. Chem. Phys.*

- 2006, 125, 74113. (c) Nakano, M.; Nitta, T.; Yamaguchi, K.; Champagne, B.; Botek, E. *J. Phys. Chem. A* **2004**, *108*, 4105. (d) Nakano, M.; Kishi, R.; Nakagawa, N.; Ohta, S.; Takahashi, H.; Furukawa, S.; Kamada, K.; Ohta, K.; Champagne, B.; Botek, E.; Yamada, S.; Yamaguchi, K. *J. Phys. Chem. A* **2006**, *110*, 4238. (e) Champagne, B.; Botek, E.; Nakano, M.; Nitta, T.; Yamaguchi, K. *J. Chem. Phys.* **2005**, *122*, 114315. (f) Champagne, B.; Botek, E.; Quinet, O.; Nakano, M.; Kishi, R.; Nitta, T.; Yamaguchi, K. *Chem. Phys. Lett.* **2005**, *407*, 372.
- (22) (a) Nakano, M.; Nagao, H.; Yamaguchi, K. *Phys. Rev. A* **1997**, *55*, 1503. (b) Nakano, M.; Yamada, S.; Yamaguchi, K. *J. Comput. Methods Sci. Eng.* **2004**, *4*, 677. (c) Nakano, M.; Yamada, S.; Kishi, R.; Takahata, M.; Nitta, T.; Yamaguchi, K. *J. Nonlinear Opt. Phys. Mater.* **2004**, *13*, 411.
- (23) (a) Nakasuji, K.; Kubo, T. *Bull. Chem. Soc. Jpn.* **2004**, *77*, 1791. (b) Nakasuji, K.; Yoshida, K.; Murata, I. *Chem. Lett.* **1982**, 969. (c) Nakasuji, K.; Yoshida, K.; Murata, I. *J. Am. Chem. Soc.* **1982**, *104*, 1432. (d) Nakasuji, K.; Yoshida, K.; Murata, I. *J. Am. Chem. Soc.* **1983**, *105*, 5136. (e) Murata, I.; Sasaki, S.; Klabunde, K.-U.; Toyoda, J.; Nakasuji, K.; Yoshida, K. *Angew. Chem., Int. Ed. Engl.* **1991**, *30*, 172. (f) Kubo, T.; Shimizu, A.; Sakamoto, M.; Uruichi, M.; Yakushi, K.; Nakano, M.; Shiomi, D.; Sato, K.; Takui, T.; Morita, Y.; Nakasuji, K. *Angew. Chem., Int. Ed.* **2005**, *44*, 6564.
- (24) (a) Nakano, M.; Kubo, T.; Kamada, K.; Ohta, K.; Kishi, R.; Ohta, S.; Nakagawa, N.; Takahashi, H.; Furukawa, S.; Morita, Y.; Nakasuji, K.; Yamaguchi, K. *Chem. Phys. Lett.* **2005**, *418*, 142. (b) Ohta, S.; Nakano, M.; Kubo, T.; Kamada, K.; Ohta, K.; Kishi, R.; Nakagawa, N.; Champagne, B.; Botek, E.; Umezaki, S.; Takebe, A.; Takahashi, H.; Furukawa, S.; Morita, Y.; Nakasuji, K.; Yamaguchi, K. *Chem. Phys. Lett.* **2005**, *420*, 432. (c) Nakano, M.; Nakagawa, N.; Ohta, S.; Kishi, R.; Kubo, T.; Kamada, K.; Ohta, K.; Champagne, B.; Botek, E.; Takahashi, H.; Furukawa, S.; Morita, Y.; Nakasuji, K.; Yamaguchi, K. *Chem. Phys. Lett.* **2006**, *429*, 174.
- (25) (a) Nakano, M.; Yamaguchi, K.; Fueno, T. *Chem. Phys. Lett.* **1991**, *185*, 550. (b) Nakano, M.; Yamada, S.; Shigemoto, I.; Yamaguchi, K. *Chem. Phys. Lett.* **1996**, *250*, 247.
- (26) (a) Herebian, D.; Wiegardt, K. E.; Neese, F. *J. Am. Chem. Soc.* **2003**, *125*, 10997. (b) Kubo, T. Doctoral thesis, Osaka University, 1996.
- (27) (a) Staroverov, V. N.; Davidson, E. R. *J. Am. Chem. Soc.* **2000**, *122*, 186. (b) Hrovat, D. A.; Duncan, J. A.; Borden, W. T. *J. Am. Chem. Soc.* **1999**, *121*, 169. (c) Flynn, C. R.; Michl, J. *J. Am. Chem. Soc.* **1974**, *96*, 3280. (d) Döhnert, D.; Kouteckoy, J. *J. Am. Chem. Soc.* **1980**, *102*, 1789. (e) Bonacic-Koutecky, V.; Koutecky, J.; Michl, J. *Angew. Chem., Int. Ed. Engl.* **1987**, *26*, 170.
- (28) (a) Jung, Y.; Head-Gordon, M. *Chem. Phys. Chem.* **2003**, *4*, 522. (b) Jung, Y.; Head-Gordon, M. *J. Phys. Chem. A* **2003**, *107*, 7475. (c) Jung, Y.; Brynda, M.; Power, P. P.; Head-Gordon, M. *J. Am. Chem. Soc.* **2006**, *128*, 7185. (d) Seierstad, M.; Kinsinger, C. R.; Cramer, C. J. *Angew. Chem., Int. Ed. Engl.* **2002**, *41*, 3894.
- (29) Yamaguchi, K. In *Self-Consistent Field: Theory and Applications*; Carbo, R.; Klobukowski, M., Eds.; Elsevier: Amsterdam, 1990; p 727.
- (30) Yamanaka, S.; Okumura, M.; Nakano, M.; Yamaguchi, K. *J. Mol. Struct. (THEOCHEM)* **1994**, *310*, 205.
- (31) Yamaguchi, K.; Okumura, M.; Takada, K.; Yamanaka, S. *Int. J. Quantum Chem. Quantum Chem. Symp.* **1993**, *27*, 501.
- (32) Cohen, H. D.; Roothaan, C. C. J. *J. Chem. Phys.* **1965**, *43*, S34.
- (33) Willetts, A.; Rice, J. E.; Burland, D. M.; Shelton, D. P. *J. Chem. Phys.* **1992**, *97*, 7590.
- (34) Kamada, K.; Ueda, M.; Nagao, H.; Tawa, K.; Sugino, T.; Shimizu, Y.; Ohta, K. *J. Phys. Chem. A* **2000**, *104*, 4723.
- (35) Frisch, M. J.; Trucks, G. W.; Schlegel, H. B.; Scuseria, G. E.; Robb, M. A.; Cheeseman, J. R.; Montgomery, J. A., Jr.; Vreven, T.; Kudin, K. N.; Burant, J. C.; Millam, J. M.; Iyengar, S. S.; Tomasi, J.; Barone, V.; Mennucci, B.; Cossi, M.; Scalmani, G.; Rega, N.; Petersson, G. A.; Nakatsuji, H.; Hada, M.; Ehara, M.; Toyota, K.; Fukuda, R.; Hasegawa, J.; Ishida, M.; Nakajima, T.; Honda, Y.; Kitao, O.; Nakai, H.; Klene, M.; Li, X.; Knox, J. E.; Hratchian, H. P.; Cross, J. B.; Bakken, V.; Adamo, C.; Jaramillo, J.; Gomperts, R.; Stratmann, R. E.; Yazyev, O.; Austin, A. J.; Cammi, R.; Pomelli, C.; Ochterski, J. W.; Ayala, P. Y.; Morokuma, K.; Voth, G. A.; Salvador, P.; Dannenberg, J. J.; Zakrzewski, V. G.; Dapprich, S.; Daniels, A. D.; Strain, M. C.; Farkas, O.; Malick, D. K.; Rabuck, A. D.; Raghavachari, K.; Foresman, J. B.; Ortiz, J. V.; Cui, Q.; Baboul, A. G.; Clifford, S.; Cioslowski, J.; Stefanov, B. B.; Liu, G.; Liashenko, A.; Piskorz, P.; Komaromi, I.; Martin, R. L.; Fox, D. J.; Keith, T.; Al-Laham, M. A.; Peng, C. Y.; Nanayakkara, A.; Challacombe, M.; Gill, P. M. W.; Johnson, B.; Chen, W.; Wong, M. W.; Gonzalez, C.; Pople, J. A. *Gaussian 03*, revision C.02; Gaussian, Inc.: Wallingford, CT, 2004.
- (36) It is well-known that the present DFT methods with conventional exchange-conventional functionals have the significant drawbacks that  $\gamma$  values are overestimated with increasing the size of  $\pi$ -conjugated systems.<sup>41</sup> Recently, the DFT method with a long-range correlation (LC) has been proposed to avoid such drawbacks. We therefore evaluate the  $\gamma$  values of IDPL, the same size phenalenyl radical system as 1 and 2, using the BLYP method with LC (LC-BLYP).<sup>42–44</sup> It turns out that the  $\gamma$  value of IDPL at the LC-BLYP/6-31G\* level of approximation is  $1902 \times 103$  au. Judging from this result in addition to the result by the UBHandHLYP method ( $\gamma = 2383 \times 103$  au),<sup>24a</sup> we predict that the overshoot of  $\gamma$  does not occur in the size of the system we discuss in this study.
- (37) Kawakami, T.; Yamanaka, S.; Takano, Y.; Yoshioka, Y.; Yamaguchi, K. *Bull. Chem. Soc. Jpn.* **1998**, *71*, 2097.
- (38) (a) Hurst, G. J. B.; Dupuis, M.; Clementi, E. *J. Chem. Phys.* **1988**, *89*, 385. (b) Maroulis, G. *J. Chem. Phys.* **1999**, *111*, 583. (c) Maroulis, G.; Xenides, D.; Hohm, U.; Loose, A. *J. Chem. Phys.* **2001**, *115*, 7957.
- (39) Salem, L.; Rowland, C. *Angew. Chem., Int. Ed. Engl.* **1972**, *11*, 92.
- (40) Bode, B. M.; Gordon, M. S. *J. Mol. Graphics Mod.* **1998**, *16*, 133.
- (41) (a) Champagne, B.; Perpète, E. A.; van Gisbergen, S. J. A.; Baerends, E.-J.; Snijders, J. G.; Soubra-Ghaoui, C.; Robins, K. A.; Kirtman, B. *J. Chem. Phys.* **1999**, *109*, 10489; Erratum **1999**, *110*, 11664. (b) van Gisbergen, S. J. A.; Schipper, P. R. T.; Gritsenko, O. V.; Baerends, E. J.; Snijders, J. G.; Champagne, B.; Kirtman, B. *Phys. Rev. Lett.* **1999**, *83*, 694. (c) Champagne, B.; Perpète, E. A.; Jacquemin, D.; van Gisbergen, S. J. A.; Baerends, E. J.; Soubra-Ghaoui, C.; Robins, K. A.; Kirtman, B. *J. Phys. Chem. A* **2000**, *104*, 4755.
- (42) (a) Iikura, H.; Tsuneda, T.; Yanai, T.; Hirao, K. *J. Chem. Phys.* **2001**, *115*, 3540. (b) Tawada, Y.; Tsuneda, T.; Yanagisawa, S.; Yanai, T.; Hirao, K. *J. Chem. Phys.* **2004**, *120*, 8425.
- (43) Becke, A. D. *Phys. Rev. A* **1988**, *38*, 3098.
- (44) Lee, C.; Yang, W.; Parr, R. G. *Phys. Rev. A* **1988**, *37*, 785.